

Diagonal Born–Oppenheimer corrections in condensed-phase ring polymer surface hopping

Cite as: J. Chem. Phys. 163, 234102 (2025); doi: 10.1063/5.0301249

Submitted: 7 September 2025 • Accepted: 25 November 2025 •

Published Online: 15 December 2025



View Online



Export Citation



CrossMark

Dil K. Limbu, Sandip Bhushal, Diana M. Castañeda-Bagatella, and Farnaz A. Shakib^{a)}

AFFILIATIONS

Department of Chemistry and Environmental Science, New Jersey Institute of Technology, Newark, New Jersey 07102, USA

^{a)}Author to whom correspondence should be addressed: shakib@njit.edu

ABSTRACT

Ring polymer surface hopping (RPSH) is a mixed quantum–classical dynamics method for incorporating nuclear quantum effects into nonadiabatic dynamics simulations via the extended phase-space of a classical ring polymer. Here, we systematically investigate several variants of RPSH in the frameworks of centroid and bead approximations (RPSH-CA and RPSH-BA) in modeling the dynamics of the spin–boson system across different reaction regimes, reorganization energies, and temperatures. Moreover, the effects of including the diagonal Born–Oppenheimer correction (DBOC) on the performance of the RPSH-CA and RPSH-BA methods are investigated. Our simulations of symmetric potentials, i.e., without energy bias, show that the RPSH-CA method, where nonadiabatic transitions are handled at the centroid level, is satisfactorily accurate and robust across different reaction regimes. Adding DBOC improves the method’s accuracy in specific intermediate and nonadiabatic reaction regimes at low temperature. Overall, the effect of DBOC in RPSH-CA is in moderation compared to the conventional fewest-switches surface hopping method where DBOC over-damps the dynamics significantly and reduces accuracy considerably, especially at low temperatures. However, the RPSH-CA and its DBOC variant struggle in simulations of asymmetric potentials especially at low temperatures. On the other hand, RPSH-BA results, where nonadiabatic transitions are handled at the level of individual beads of the ring polymers, are generally unreliable unless in the high temperature adiabatic reaction regimes with symmetric potentials. The inclusion of DBOC is not particularly helpful in remedying this erratic behavior. Our findings clarify when geometric corrections are beneficial or detrimental to nonadiabatic simulations using RPSH, providing practical guidance for atomistic condensed-phase applications.

Published under an exclusive license by AIP Publishing. <https://doi.org/10.1063/5.0301249>

I. INTRODUCTION

Path integral formalism of quantum mechanics^{1,2} achieves the preservation of the quantum Boltzmann distribution via an isomorphic classical Hamiltonian.³ This feat is highlighted in the development of approximate methods, centroid molecular dynamics (CMD)^{4–7} and ring polymer MD (RPMD),^{8–10} for investigating chemical dynamics on a single electronic surface.^{11–14} Nuclear quantum effects (NQEs), such as zero-point energy and tunneling, are included in adiabatic dynamics simulations via the extended phase-space of a ring polymer created from n replicas of the physical system, also known as beads, coupled by harmonic forces. While RPMD and CMD are not derived from first principles, they can be recovered from Matsubara dynamics with a generalized Kubo-transformed time correlation function formalism,¹⁵ putting them

on a strong ground for further developments beyond the adiabatic reaction regime.^{16,17}

RPMD formalism has been successfully utilized in the description of electron transfer¹⁸ and proton-coupled electron transfer¹⁹ reactions. Despite its success, the computational cost associated with quantizing both nuclear and electronic degrees of freedom by ring polymers, with more than 1000 beads needed for the latter,^{18,19} renders this treatment expensive for multi-electron/multi-proton non-adiabatic dynamics simulations. However, inclusion of NQEs via the extended phase-space of a ring polymer is more affordable than other sophisticated methods, such as the mixed quantum classical Liouville approach^{20–22} where both proton and electron wavefunctions need to be expanded in terms of harmonic basis sets on top of the millions of trajectories needed to be run for convergence.^{23–25} Among multi-state RPMD formulations, ring polymer surface

hopping (RPSH)^{26,27} stands out for its simplicity, ease of implementation, and inherent capability of the method for including NQEs into nonadiabatic MD simulations. Describing the nonadiabatic electronic transitions according to the fewest switching surface hopping (FSSH)^{28–30} algorithm, RPSH is conveniently suitable for multi-electron nonadiabatic dynamics simulations. In a different class than nonadiabatic instanton theory^{31–33} and mean-field RPMD,^{34,35} it does not rely on a thermally averaged description of the electronic nonadiabatic dynamics but follows the dynamics explicitly on each adiabatic surface, making it more suitable for simulating scattering events and calculating branching probabilities. Finally, as in the original FSSH, the quantum wave-packet is propagated along the classical trajectories, and the latter are apportioned among different electronic surfaces according to quantum amplitudes. Hence, the RPSH algorithm carries quantum phase and accounts for electronic coherence.

Recent advancements have been reported for RPSH via propagating the dynamics subject to a generalized Hamiltonian,³⁶ weighted bead-averaged probability of nonadiabatic transitions,³⁷ and capturing electronic decoherence.³⁸ In addition, recent refinement schemes have focused on improving sampling strategies,^{39,40} correcting description of electronic coherence,^{41,42} and preserving quantum Boltzmann distribution by proper treatment of classically forbidden transitions.⁴³ In the light of the increasing attention to the RPSH simulations and for the purpose of systematically improving the method, here we evaluate the performance of RPSH in the frameworks of both centroid and bead approximations (RPSH-CA and RPSH-BA, respectively)²⁶ in condensed-phase dynamics simulations and investigate the effect of combining them with the diagonal Born–Oppenheimer correction (DBOC).

DBOC, as the second-order derivative coupling of electronic wavefunction, is a diagonal term that arbitrarily modifies the BO potential energy surface (PES). It is often neglected in simulations based on mixed quantum–classical dynamics methods due to the absence of a nuclear wavepacket in such schemes.⁴⁴ Nevertheless, the inclusion of the DBOC in surface hopping methods has been advocated at least for regions with significant nonadiabatic couplings.^{45,46} At the same time, other studies have cautioned about its usage.⁴⁷ It is shown that by adding a repulsive wall in the regions where the two surfaces come close to each other, DBOC deteriorates the results of FSSH simulations.⁴⁸ In comparison, inclusion of NQEs within the RPSH framework, which allows tunneling through an energy barrier, can lead to a different effect than in FSSH. While it would modify the shape of the PESs, the final outcome of the simulations would be dictated by an interrelation between the magnitude of DBOC, the possibility of tunneling via the energy barrier, and the probability of nonadiabatic transitions.

In this work, we first evaluate the performance of RPSH-CA and RPSH-BA on a generic two-level system coupled to a classical bath with arbitrary coupling strengths as in the spin-boson model. This model system allows us to probe the capability of the RPSH methods in modeling the population relaxation and preserving quantum Boltzmann distribution in condensed-phase simulations. Then, DBOC will be explicitly incorporated into both frameworks. In the remainder of this paper, we first give a brief summary of the RPSH-CA and RPSH-BA algorithms as well as methodological considerations regarding improvements of the method. The chosen approach for the inclusion of DBOC in RPSH, as well as the

studied model, will also be introduced in Sec. II. Section III will present results and discussions for dynamics simulations at high and low temperature limits (300 vs 30 K) in the context of the spin-boson model, and comparisons will be made to the original FSSH as well as its DBOC-added variant. Concluding remarks and our outlook toward future research directions in this field will be presented in Sec. IV.

II. THEORY

A. Ring polymer surface hopping from centroid and bead perspectives

For a system of N particles in the electronic ground state, the general Hamiltonian is written as

$$\hat{H} = \sum_{I=1}^N \frac{\hat{\mathbf{P}}_I^2}{2M_I} + \hat{V}(\mathbf{R}), \quad (1)$$

where \mathbf{R} and \mathbf{P} are position and momentum vectors, respectively, M_I is the mass of the I th nuclear degree of freedom (DOF), and $\hat{V}(\mathbf{R})$ is the potential energy surface. The path integral discretization of the quantum mechanical canonical partition function^{2,3,49} of this system yields

$$Z = \text{Tr} [e^{-\beta \hat{H}}] = \lim_{n \rightarrow \infty} \frac{1}{(2\pi\hbar)^f} \int d^f \mathbf{R} \int d^f \mathbf{P} e^{-\beta_n H_n(\mathbf{R}, \mathbf{P})}, \quad (2)$$

where $f = Nn$ and n is the number of imaginary time slices, or “beads,” of the path integral, and $\beta_n = \beta/n$, with $\beta = (k_B T)^{-1}$ being the reciprocal temperature. The extended Hamiltonian, H_n , is associated with the positions, $\mathbf{R} = \{\mathbf{R}_1, \dots, \mathbf{R}_n\}$, and momenta, $\mathbf{P} = \{\mathbf{P}_1, \dots, \mathbf{P}_n\}$, vectors of the ring polymer and is defined as

$$H_n(\mathbf{R}, \mathbf{P}) = \sum_{I=1}^N \sum_{j=1}^n \left[\frac{P_{I,j}^2}{2M_I} + \frac{1}{2} M_I \omega_n^2 (R_{I,j} - R_{I,j-1})^2 \right] + \sum_{j=1}^n V(R_{1,j}, \dots, R_{N,j}). \quad (3)$$

The definition of mass in the fictitious kinetic energy term constructs one of the two fundamental differences between running the dynamics with RPMD⁸ vs obtaining statistical information from the path integral molecular dynamics (PIMD).³ The former uses the physical mass of each bead, where the latter may use a fictitious mass. The second term in Eq. (3) represents the harmonic interaction between adjacent beads with $\omega_n = 1/\beta_n \hbar$.

Surface hopping approach can take advantage of the extended Hamiltonian in Eq. (3) for propagating the dynamics of the whole ring polymer on a single adiabatic surface $|\alpha; \mathbf{R}\rangle$, where the fewest switches ansatz would take it from one surface to another. The only change that is made to the Hamiltonian is introducing the state-dependent potentials as $V_\alpha(\mathbf{R}) = \langle \alpha; \mathbf{R} | \hat{V} | \alpha; \mathbf{R} \rangle$, giving birth to the RPSH algorithm. Surface-hopping algorithm requires the numerical integration of the time-dependent Schrödinger equation (TDSE) along the motion of classical trajectories. Originally, two alternative approximations were proposed for this integration in the context of RPSH.²⁶ In bead-averaged approximation, i.e., RPSH-BA, TDSE takes the form

$$i\hbar \dot{c}_\alpha(t) = \left[\frac{1}{n} \sum_{j=1}^n V_\alpha(\mathbf{R}_j) \right] c_\alpha - i\hbar \sum_\beta \left[\frac{1}{n} \sum_{j=1}^n \dot{\mathbf{R}}_j \cdot \mathbf{d}_{\alpha\beta}(\mathbf{R}_j) \right] c_\beta(t), \quad (4)$$

where $c_\alpha(t)$ are the time-dependent complex expansion coefficients of the adiabatic basis and $\mathbf{d}_{\alpha\beta}(\mathbf{R}_j) = \langle \alpha; \mathbf{R}_j | \nabla_{\mathbf{R}_j} | \beta; \mathbf{R}_j \rangle$ is the nonadiabatic coupling vector (NACV) between surfaces with respect to the position of each bead of the ring polymer.

Alternatively, in the centroid approximation, i.e., RPSH-CA, the position and momentum of the centroid of the ring polymer are updated at every time step of the nuclear dynamics, as

$$\bar{\mathbf{R}} = \frac{1}{n} \sum_{j=1}^n \mathbf{R}_j, \quad \bar{\mathbf{P}} = \frac{1}{n} \sum_{j=1}^n \mathbf{P}_j. \quad (5)$$

Then, TDSE is numerically integrated as

$$i\hbar \dot{c}_\alpha(t) = V_\alpha(\bar{\mathbf{R}}) c_\alpha(t) - i\hbar \sum_\beta \dot{\bar{\mathbf{R}}} \cdot \mathbf{d}_{\alpha\beta}(\bar{\mathbf{R}}) c_\beta(t), \quad (6)$$

where both the energy of the adiabatic surfaces, $V_\alpha(\bar{\mathbf{R}})$, and the NACV between surfaces, $\mathbf{d}_{\alpha\beta}(\bar{\mathbf{R}}) = \langle \alpha; \bar{\mathbf{R}} | \nabla_{\bar{\mathbf{R}}} | \beta; \bar{\mathbf{R}} \rangle$, are evaluated at the centroid level.

The probability of the nonadiabatic transition between surfaces at each time step is defined based on density matrix elements, $\rho_{\alpha\beta} = c_\alpha c_\beta^*$, and the associated derivative coupling. If the transition occurs, the entire ring polymer switches to the new state, and the kinetic energy is accordingly adjusted to conserve the total energy for an RPSH trajectory.

B. Theoretical considerations about the RPSH formalism

Here, instead of providing the details of the algorithms, which are available elsewhere,^{26,27,43} we discuss and clarify some aspects of RPSH for condensed-phase nonadiabatic simulations.

- During RPSH simulations, we keep the whole ring polymer confined to one electronic state instead of assigning state-specific indices to the beads and spreading the ring polymer over different states. In fact, the latter has already been investigated in a slightly different flavor of RPSH algorithm.³⁹ While the method was validated numerically, it was inefficient in sampling the off-diagonal elements of observables related to the coupling of different states. This was due to the fact that the major contributors to these elements were configurations with kinks, i.e., consecutive beads residing on different surfaces, and they had a higher energy than configurations without kinks. Allowing an infinite number of switches resulted in a proper sampling of these rare events, but it simply converged the method⁴⁰ to a mean-field ring polymer representation. This is the same observation that led to development of FSSH algorithm where the number of state switches should be minimized to maintain the correct statistical distribution of state populations,²⁹ otherwise the algorithm would regress to a mean-field-like dynamics simulation. Evolving the ring polymer on one surface in RPSH avoids such sampling issues and preserves a surface hopping algorithm suitable for simulating branching and scattering events.

- It is accustomed in RPMD simulations that the classical ring polymer Hamiltonian is sampled at an elevated temperature of β_n instead of the real temperature β . This ensures the positions of all beads are distributed according to the exact quantum Boltzmann distribution.^{8,16} However, multi-state RPSH is different from adiabatic RPMD in that partitioning of trajectories on different electronic states is mainly dictated by the surface hopping algorithm. Using a two-level system coupled to a chain of classical particles, we have shown that RPSH-CA *approximately* reproduces the correct Boltzmann populations subject to a proper treatment of classically forbidden transitions, also known as frustrated hops.⁴³ This puts the method in a different class than most other multi-state RPMD methods, which fail to reproduce the expected Boltzmann populations, in part due to zero-point energy leakage.¹⁷ Here, we reverse the velocity of frustrated hops along the direction of NACVs at the centroid level to help preserve the quantum Boltzmann distribution. Alternatively, as we have shown before, one can rescale the velocity along the direction of NACVs of each bead of the ring polymers, leading to slightly different results.²⁷ That being said, we remind the readers of our previous studies, where we caution about the possible adverse effect of reversing the velocity of frustrated hops on the quantum dynamics in different model systems.⁴³

- The RPSH results in the current study are not corrected for the lack of decoherence or the overcoherence problem of the surface hopping algorithm. A very detailed and comprehensive study on the effect of decoherence correction in simulating the nonadiabatic dynamics of the spin-boson model using the FSSH method has already been carried out by Chen and Reichman.⁵⁰ Correcting the non-equilibrium dynamics, either with the augmented FSSH (A-FSSH) method⁵¹ or simply damping the coherence of the density matrix via a pure-dephasing-like rate,⁵² clearly did very little for improving the results.⁵⁰ Generally, A-FSSH produces a similar population transfer profile to FSSH whereas dephasing damps the oscillatory population decays without necessarily improving the results. On the other hand, other studies have probed the effect of decoherence correction in RPSH and reported promising results for 1D Tully models.³⁸ However, the lack of a well-defined temperature in such models and the variety of decoherence-correction approaches may require a more comprehensive study in the future.

C. Diagonal Born-Oppenheimer correction

The action of the nuclear kinetic energy operator, $\hat{T}_n = -\sum_I \frac{\hbar^2}{2M_I} \nabla_{\mathbf{R}_I}^2$, on the adiabatic electronic wavefunctions results in diagonal and off-diagonal nonadiabatic couplings.^{48,53} The former is a potential-like term and will modify the adiabatic PESs, $V_\alpha(\mathbf{R})$, as

$$\tilde{V}_\alpha(\mathbf{R}) = V_\alpha(\mathbf{R}) + V_{\text{DBOC}}^{(\alpha)}(\mathbf{R}). \quad (7)$$

The correction term for N ring polymers comprised of n beads is defined as

$$V_{\text{DBOC}}^{(\alpha)}(\mathbf{R}) = \sum_{I=1}^N \frac{\hbar^2}{2M_I} \sum_{j=1}^n \sum_{\beta \neq \alpha} |\mathbf{d}_{I,j}^{(\alpha\beta)}(\mathbf{R}_j)|^2. \quad (8)$$

The total force acting on bead j on adiabatic state α is given by

$$\mathbf{F}_{I,j} = -\nabla V_{\alpha}(\mathbf{R}_j) = -\nabla V_{\alpha}(\mathbf{R}_j) - \nabla V_{\text{DBOC}}^{(\alpha)}(\mathbf{R}_j) = \mathbf{F}_{I,j}^{(0)} + \Delta\mathbf{F}_{I,j}, \quad (9)$$

where $\mathbf{F}_{I,j}^{(0)}$ is the original force without the correction and the DBOC force contribution is given by

$$\Delta\mathbf{F}_{I,j} = \sum_{\alpha \neq \beta} \frac{1}{M_I} \mathbf{d}_{I,j}^{(\alpha\beta)}(\mathbf{R}_j) \cdot \nabla \mathbf{d}_{I,j}^{(\alpha\beta)}(\mathbf{R}_j). \quad (10)$$

The NACVs are computed at the individual bead level of the ring polymers according to

$$\mathbf{d}_{I,j}^{(\alpha\beta)} = \frac{\langle \psi_{j,\alpha} | \nabla_{R_{I,j}} H(\mathbf{R}_j) | \psi_{j,\beta} \rangle}{V_{\beta}(\mathbf{R}_j) - V_{\alpha}(\mathbf{R}_j)}. \quad (11)$$

In this work, DBOC forces are computed numerically via the finite difference method according to

$$\nabla \mathbf{d}_{I,j}^{(\alpha\beta)} = \frac{\mathbf{d}_{I,j}^{(\alpha\beta)}(\mathbf{R}_j + \delta) - \mathbf{d}_{I,j}^{(\alpha\beta)}(\mathbf{R}_j - \delta)}{2\delta}. \quad (12)$$

The displacement parameter δ should be chosen carefully to ensure numerical stability and convergence of the DBOC forces within the dynamics simulations.

D. Simulation details

The spin-boson model is a well-known system that offers a theoretical framework for examining nonadiabatic dynamics in a condensed phase environment.⁵⁴ Details of the model, including discretizations of the bath,^{55,56} are provided in the [supplementary material](#), Secs. S1–S3 and Fig. S1. Our RPSH schemes investigate the nonadiabatic dynamics of N classical bath trajectories, all of which are represented with ring polymers composed of n beads. Initial nuclear positions and momenta can be sampled from a normal distribution,

$$\rho(\mathbf{R}, \mathbf{P}) = \prod_{I=1}^N \prod_{j=1}^n \exp \left[-\beta_n \left(\frac{P_{I,j}^2}{2M_I} + \frac{1}{2} M_I \omega_I^2 R_{I,j}^2 \right) \right], \quad (13)$$

where ω_I is the frequency of the I th bath mode. Alternatively, one can employ a normal mode distribution for the ring polymer,

$$\rho_{\text{RP}}(\tilde{\mathbf{R}}, \tilde{\mathbf{P}}) = \prod_{I=1}^N \prod_{k=1}^n \exp \left[-\beta_n \left(\frac{\tilde{P}_{I,k}^2}{2M_I} + \frac{1}{2} M_I \omega_{I,k}^2 \tilde{R}_{I,k}^2 \right) \right], \quad (14)$$

where $\omega_{I,k}^2 = \omega_I^2 + \omega_k^2$, with ω_I being the frequency of the I th bath mode and ω_k being the frequency of the k th normal mode. These coordinates can be transformed back to primitive bead coordinates via the inverse normal mode transformation. With proper implementation, these two initial sampling methods should yield similar results. Here, the initial nuclear positions and momenta are sampled from a normal mode distribution consistent with the ring polymer representation as in Eq. (14).

All simulations are carried out using 10 000 independent trajectories, each coupled to a Debye spectral bath^{57,58} consisting of 100 harmonic oscillator modes. The bath frequencies are sampled according to a Debye spectral density^{59–61} with appropriate reorganization energy^{62,63} and cutoff frequency. Trajectories are propagated for 0.5 ps using a time step of 0.0242 fs (1 a.u.). The initial electronic wave packet is prepared and projected onto the adiabatic basis, and the initial active surface, λ , is selected based on initial electronic amplitudes, i.e., trajectories are placed on surface α with probability $|c_{\alpha}|^2$. Diabatic populations are computed on-the-fly using the mixed quantum–classical density matrix formalism, as described in Ref. 64,

$$P_D = \left\langle \sum_{\alpha} |U_{D\alpha}|^2 \delta_{\alpha,\lambda} + \sum_{\alpha < \beta} 2 \operatorname{Re}[U_{D\alpha} c_{\alpha} c_{\beta}^* U_{D\beta}^*] \right\rangle, \quad (15)$$

where $U_{D\alpha}$ are elements of the adiabatic-to-diabatic transformation matrix, λ denotes the active surface, and $\rho_{\alpha\beta} = c_{\alpha} c_{\beta}^*$ is the electronic density matrix. Final populations are obtained by averaging over the full ensemble of trajectories.

III. RESULTS AND DISCUSSION

We systematically evaluate the applicability of RPSH in condensed-phase dynamics simulations by investigating population dynamics of first symmetric and then asymmetric spin-boson models across various temperatures, reorganization energies, E_r , and reaction regimes. At the same time, we assess the effect of incorporating DBOC within the RPSH framework. Exact quantum results based on the hierarchical equations of motion (HEOM)^{65,66} are computed using QuTiP⁶⁷ and serve as benchmarks throughout. All the RPSH simulations are conducted using 32 beads, including RPSH-CA and RPSH-BA, as well as their new variants with DBOC, namely, RPSH-CA^D and RPSH-BA^D, respectively, with the superscript D denoting the inclusion of DBOC terms. Convergence of results with respect to the number of beads is shown for intermediate and nonadiabatic reaction regimes and low-temperature limits in the [supplementary material](#), Figs. S2 and S3. Note that this number of beads is only followed for the sake of consistency in the current paper. For most reaction regimes, such as the adiabatic reaction regime at high or low temperature, the results are already converged with only four beads. All the simulations are carried out up to 0.5 ps. By definition, the original RPMD method is expected to produce exact quantum dynamical properties at the limit that time goes to zero ($t \rightarrow 0$), albeit as $n \rightarrow \infty$.⁸ In the current work, we refer to the time limit closer to zero as short-time and the time limit closer to 0.5 ps as long-time limits. With this distinction, we investigate how the RPSH method fares moving away from the $t \rightarrow 0$ limit.

A. Symmetric spin-boson nonadiabatic dynamics

Figure 1 shows the change of population of the donor diabatic electronic state (P_D) at a high temperature of 300 K. The population dynamics of the spin-boson model is reported for three reorganization energies: $E_r = 0.02$, $E_r = 1$, and $E_r = 5$, each examined in adiabatic ($\Delta/\omega_c > 1$), intermediate ($\Delta/\omega_c = 1$), and nonadiabatic ($\Delta/\omega_c < 1$) reaction regimes. These reaction regimes correspond to slow, comparable, and fast motions of bath relative to the electronic coupling, Δ , respectively.

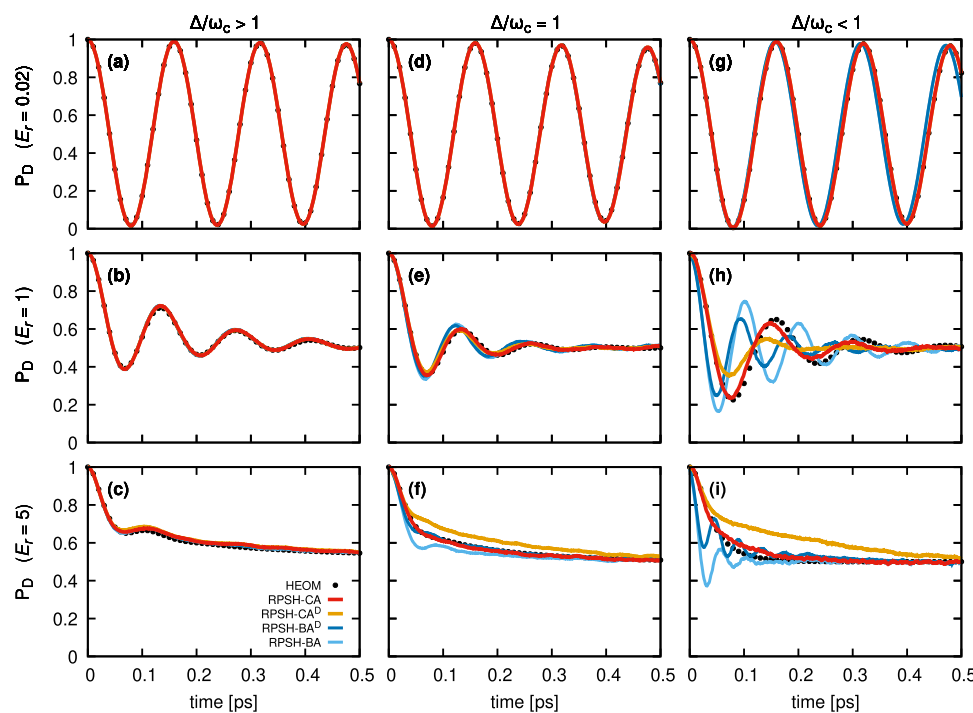


FIG. 1. Population dynamics for the spin-boson model at the high temperature of 300 K and three reorganization energies, $E_r = 0.02$ (top row), $E_r = 1$ (middle row), and $E_r = 5$ (bottom row), across different reaction regimes (columns). Model parameters include $\varepsilon = 0$, $\Delta = 1.0$, and $\omega_c = \{0.25\Delta, \Delta, 5\Delta\}$. All energies are in the unit of 104.25 cm^{-1} .

As shown in Fig. 1(a), there is an excellent agreement between the simulated population dynamics using four RPSH variants and the exact quantum results in the adiabatic reaction regime. Coherence, oscillation amplitude, and phase align closely with HEOM benchmarks. As the coupling of the quantum sub-system to the classical solvent increases, Figs. 1(a)–1(c), all four methods keep performing very well in reproducing exact results.

Figures 1(d)–1(f) demonstrate the population transfer profile in the intermediate reaction regime where all four methods are exact at $E_r = 0.02$. As the reorganization energy increases, RPSH-CA remains very reliable, producing quantum populations close to exact results. RPSH-BA starts showing small deviations from exact results, more apparent at the highest degree of coupling to the bath, Fig. 1(f), while RPSH-BA^D improves the performance to a great deal. On the other hand, DBOC inclusion has a deteriorating effect on the performance of RPSH-CA in this regime; compare the yellow vs red lines shown in Fig. 1(f).

Figures 1(g)–1(i) demonstrate the population transfer profile in the nonadiabatic reaction regime. Here, RPSH-BA shows deviations from the exact results at all values of E_r , while RPSH-CA performs satisfactorily well in reproducing the correct phase oscillation in the short-time limit and the Boltzmann populations at the long-time limit as E_r increases. The diagonal correction adds a repulsive wall to the ground state adiabatic PES when the energy of the two states gets close, thus hindering the population transfer from the donor to the acceptor side. This leads to a deteriorating effect on the P_D profile in RPSH-CA^D. However, the same change of PES has an improving effect on RPSH-BA, which was already suffering from an exaggerated population transfer from reactant to product. As a result, in comparison with RPSH-BA, RPSH-BA^D produces better

agreement with the exact results in terms of the amplitude of population oscillation, but is still unreliable in terms of correct phase oscillations.

Figure 2 demonstrates the population transfer profile of the spin-boson model at different reaction regimes at a low temperature of 30 K. The population dynamics are presented for the same set of reorganization energies: $E_r = 0.02$, $E_r = 1$, and $E_r = 5$, analyzed under slow, intermediate, and fast bath motions. Here, the adiabatic reaction regime with the lowest E_r of 0.02, Figs. 2(a), 2(d), and 2(g), is where all four methods work very well in accordance with exact simulations. Increasing the reorganization energy to $E_r = 1$ in Fig. 2(b), RPSH-CA and RPSH-CA^D preserve the correct Rabi oscillations in the 0.5 ps time frame, while the amplitudes of the population oscillations become higher than the exact results as the time goes on. On the other hand, RPSH-BA and RPSH-BA^D show deviation from both amplitude and phase of oscillations as time goes on. Nevertheless, all methods work satisfactorily in these regimes at the short-time limit. At the highest reorganization energy of $E_r = 5$, Fig. 2(c), all methods show deviations from correct oscillations.

The effect of inclusion of DBOC in RPSH is more apparent in intermediate and nonadiabatic reaction regimes with higher reorganization energies of $E_r = 1$, Figs. 2(e) and 2(h), and $E_r = 5$, Figs. 2(f) and 2(i). However, we first need to discuss the elephant in the room, which is the nonphysical oscillatory behavior of RPSH-BA and RPSH-BA^D in these reaction regimes. A comparison of the nonadiabatic transition statistics over 10 000 RPSH-CA and RPSH-BA trajectories shows a similar frequency of successful or frustrated hops in almost all reaction regimes at both high and low temperature; see Figs. S4 and S5 in the [supplementary material](#). The slight differences of the frequencies of hops in the high reorganization

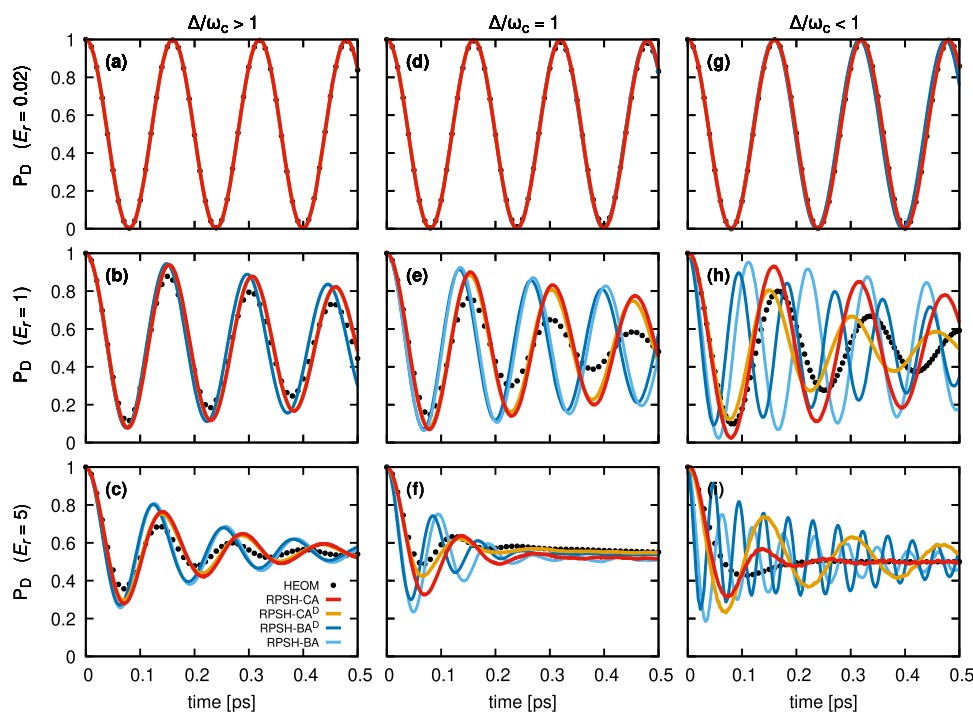


FIG. 2. Population dynamics of the spin-boson model at the low temperature of 30 K for three reorganization energies and different reaction regimes. All the model parameters are the same as in Fig. 1.

energy and nonadiabatic reaction regime cannot explain the very clear difference in the behavior of RPSH-BA vs RPSH-CA seen here. Note that the diabatic donor populations are computed using the mixed quantum-classical density matrix formalism in Eq. (15), which in turn is dominated by the time evolution of the electronic state coefficients via Eq. (4) in RPSH-BA and Eq. (6) in RPSH-CA. Figures S6(a)–S6(c) in the [supplementary material](#) show the time evolution of c_α for the same trajectory in RPSH-BA vs RPSH-CA. As can be seen, the former shows very intense oscillations compared to the smooth behavior of the latter. Taking the averages over the quantities of each of the 32 beads of all 100 classical ring polymers, randomly distributed over the electronic PESs, leads to this oscillatory behavior, whereas the narrower distribution of the centroids of ring polymers leads to a smooth behavior free from nonphysical oscillations. It should be mentioned that this difference between RPSH-BA and RPSH-CA is seen due to the high number of classical DOFs and the disparate spatial distributions of different ring polymers. Such an observation would not be apparent in the earlier studies of RPSH, which involved only one classical DOF.²⁶ This issue can be shown even here by reducing the number of beads of ring polymers from 32 to 4, Figs. S6(d)–S6(f) in the [supplementary material](#), which leads to more tamed oscillations of the electronic coefficients over time in RPSH-BA while it does not have such a pronounced effect on RPSH-CA.

Based on these observations, here we will only discuss the effect of DBOC on RPSH-CA while cautioning the community about using RPSH-BA for inclusion of NQEs into the condensed-phase MD simulations at low temperature limits despite the early reports on its success²⁶ in 1D scattering models. At the highest reorganization energy of the intermediate reaction regime, Fig. 2(f),

RPSH-CA^D acts more reliably in capturing the correct population profile in comparison with the original RPSH-CA. In $E_r = 1$ in the nonadiabatic reaction regime, Fig. 2(h), the damped dynamics of RPSH-CA^D, due to the repulsive wall on the PES, corrects the overestimation of population transfer happening in RPSH-CA. As a result, RPSH-CA^D reproduces the correct population amplitude, albeit with shifted oscillations. Figure 2(i) shows the population transfer profile at $E_r = 5$ in the nonadiabatic reaction regime. Here, RPSH-CA is very successful in reproducing the quantum population in the long-time limit. However, it faces nonphysical oscillations in the short-time limit. These oscillations, which become more apparent in RPSH-CA^D, can be the result of internal high-frequency oscillations of the ring polymers affected by the number of beads. Figure S2(d) in the [supplementary material](#) shows that using four beads instead of 32 beads would smooth out such oscillations in RPSH-CA, still preserving correct population in the long-time limit.

B. Asymmetric spin-boson nonadiabatic dynamics

The asymmetric spin-boson model with a Debye bath presents a more stringent benchmark for any approximate quantum dynamics method than the symmetric case due to the inherent energy bias between diabatic states.^{68–70} On a related note, the original RPMD has an inferior performance in an anharmonic potential than the harmonic potential.⁸ Hence, it is interesting to see the performance of RPSH in challenging cases such as asymmetric spin-boson model. Figure 3 compares the performance of RPSH-CA, RPSH-CA^D, RPSH-BA, and RPSH-BA^D against exact HEOM dynamics at 300 and 30 K for $\varepsilon = 1$, $\Delta = 1$, and under the lowest and highest reorganization energies of $E_r = 0.02$ and 5. The results cover

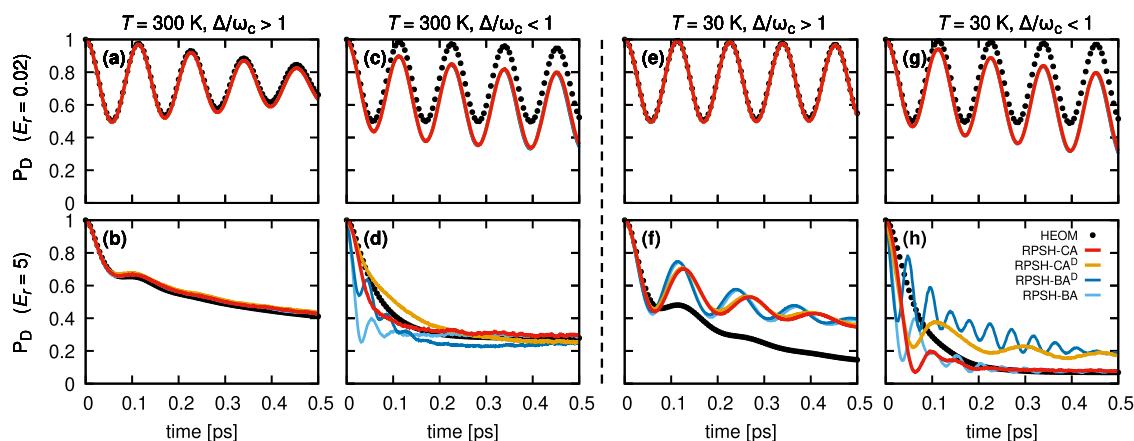


FIG. 3. Population dynamics of the asymmetric spin-boson model at 300 K [(a)–(d), left panel] and 30 K [(e)–(h), right panel] for low and high reorganization energies: $E_r = 0.02$, top panels, and $E_r = 5$, bottom panels, spanning both adiabatic and nonadiabatic reaction regimes. The results from RPSH-CA and RPSH-BA and their DBOC variants (RPSH-CA^D and RPSH-BA^D) are compared against exact quantum dynamics results. Here, $\epsilon = 1.0$ and all other model parameters are the same as shown in Fig. 1.

adiabatic and nonadiabatic reaction regimes with $\omega_c = 0.25$ and 5. At high temperature and slow bath motion, all methods reproduce the overall relaxation and equilibrium populations with good accuracy at both $E_r = 0.02$ and 5, as shown in Figs. 3(a) and 3(b). However, stark deviations occur at both cases with the fast bath motions. With $E_r = 0.02$, all four methods similarly deviate from the exact behavior, as shown in Fig. 3(c). With $E_r = 5$, while they perform poorly at the shot-time limit, they recover toward the long-time limit. At the low temperature limit, we notice poorer performance from RPSH. Figure 3(e) presents an exact performance by all methods at the adiabatic reaction regime and the lowest coupling to the environment. However, increasing E_r to 5, all methods completely fail in reproducing the correct population transfer profile. Their performance is not much better in the nonadiabatic reaction regime with the exception of RPSH-CA and, surprisingly, RPSH-BA being able to retrieve correct Boltzmann population at $E_r = 5$, Fig. 3(h). Overall, in the studied asymmetric models, the DBOC inclusion provided no improvements in the obtained results.

C. DBOC effect in RPSH vs FSSH

Focusing on the nonadiabatic reaction regime, with high reorganization energies of 1 and 5, Fig. 4 compares and contrasts the performance of RPSH-CA and RPSH-CA^D to the classical FSSH and its DBOC variant (FSSH^D) at a low temperature of 30 K. The comparison is made in both symmetric, Figs. 4(a) and 4(b), and asymmetric, Figs. 4(c) and 4(d), cases. As can be seen in Figs. 4(a) and 4(c), both RPSH-CA and FSSH perform poorly in reproducing the population transfer profile at $E_r = 1$. However, in the symmetric potential, RPSH-CA^D recovers the correct amplitude of population oscillations but not the phase. In the same region, DBOC has a completely deteriorating effect on FSSH results. It can be inferred that, in accordance with the literature,^{47,48} the DBOC repulsive wall on PES at the barrier crossing hinders the population transfer between the donor and the acceptor sites in the FSSH^D simulations. However, RPSH-CA^D encounters a smoother change of the shape of the PES

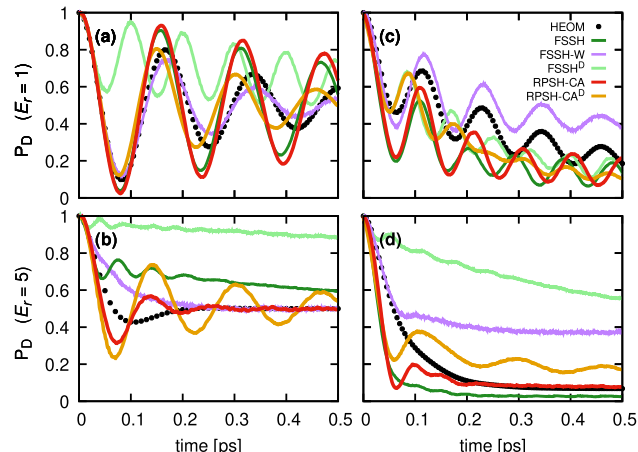


FIG. 4. Population dynamics of the symmetric [(a) and (b)] and asymmetric [(c) and (d)] spin-boson models at a low temperature of 30 K, shown for different reorganization energies in the nonadiabatic reaction regime ($\omega_c = 5\Delta$). The plots compare results from FSSH, RPSH, their DBOC-corrected variants (FSSH^D and RPSH-CA^D), and FSSH initialized from a Wigner distribution (FSSH-W) against exact results.

due to the distribution of ring polymers, which does not hinder the population transfer as in the case of FSSH. In the asymmetric case, while DBOC seems to shift both RPSH-CA and FSSH populations toward the exact results, it does not leave a lasting improving effect on either method.

As the reorganization energy increases to $E_r = 5$ in Figs. 4(b) and 4(d), FSSH fails to reproduce the correct population transfer profile while the DBOC variant has an even more devastating effect on the results. Obviously, the repulsive wall on the PES completely dampens the population transfer between the donor and acceptor sites. On the other hand, in both symmetric and asymmetric

cases, RPSH-CA is capable of reproducing the long-time Boltzmann population even though showing nonphysical oscillations in the short-time limit. Overall, the deteriorating effect of DBOC on the RPSH-CA results is not as extreme as the FSSH case. One might even argue that the nonphysical oscillations in RPSH-CA^D can be damped with a proper decoherence scheme, leading to more improved results.

To be more precise about the effect of DBOC in RPSH vs FSSH, we repeat that the height of the DBOC repulsive wall on adiabatic PESs in RPSH-CA^D cannot be as high as the case in FSSH^D. The DBOC in RPSH-CA^D is calculated based on Eq. (8), which takes the average of NACVs of all beads of the ring polymers. Since the corresponding NACVs of different beads spike at slightly different positions, taking the average leads to a smoother change of the shape of PESs compared to one NACV in a classical FSSH trajectory. This point is more clarified in a test-case study where we calculate DBOC for RPSH-CA^D at the centroid level instead of every bead of the ring polymers. Since the centroid is like one individual classical particle, the DBO correction of RPSH-CA at the centroid level leads to a very steep repulsive potential wall and basically similar results to FSSH^D; see Fig. S7 in the [supplementary material](#). Overall, it can be said that the RPSH-CA^D method either improves the RPSH-CA results or, at least, does not diminish them to the degree that happens in the FSSH method. Therefore, we suggest DBOC as a parameter that is worth testing when dealing with different systems of interest, the results of which, of course, are method-dependent.

Finally, Fig. 4 also demonstrates FSSH populations initialized from a Wigner distribution (FSSH-W) to assess the influence of the initial nuclear distribution on its performance. As can be seen, FSSH-W yields some improvement over standard FSSH, particularly in the short-time dynamics where the initial quantum distribution plays a role in capturing NQEs. For the moderate reorganization energy case ($E_r = 1$), FSSH-W captures the correct phase oscillations but deviates from the exact population amplitude in the long-time limit. This is specifically apparent in the asymmetric case shown in Fig. 4(c). In the strong reorganization energy regime, $E_r = 5$, FSSH-W shows similar behavior to RPSH-CA in symmetric potential, Fig. 4(b). However, its shortcoming in reproducing the long-time dynamics due to zero-point energy leakage⁷¹ is apparent in the asymmetric potential, Fig. 4(d). In comparison, the power of RPSH-CA comes from improved dynamics due to capturing NQEs via the extended phase-space of ring polymers and not from the specific choice of initial distribution. This point is of utmost importance in simulating realistic systems with many coupled DOFs since the Wigner transform cannot be obtained analytically for such systems.

IV. CONCLUSIONS AND OUTLOOKS

In this study, we developed and tested different RPSH methods that incorporate the diagonal Born–Oppenheimer correction alongside derivative couplings into nonadiabatic MD simulations, focusing on the spin-boson model as a benchmark. We employed two different versions of RPSH, where nonadiabatic transitions are captured at the centroid or bead level, RPSH-CA and RPSH-BA, respectively. By comparing these methods and the standard FSSH with their DBOC-included variants across various reorganization energies and reaction regimes, we systematically explored the influence of geometric corrections on quantum dynamics. Our results,

overall, demonstrate the utility of RPSH methods for condensed-phase MD simulations at physically meaningful temperatures. It is a step forward in the utilization of RPSH in comparison with 1D model systems with arbitrary temperatures employed previously. Across most reaction regimes examined in a symmetric potential, RPSH-CA consistently preserves quantum coherence and maintains satisfactory oscillation amplitude and phase, even under strong system–bath coupling strengths. In some reaction regimes, the addition of DBOC can further improve the accuracy of RPSH-CA results. On the other hand, RPSH-BA and its DBOC variant deviate considerably from correct dynamics behavior at the low temperature of 30 K unless in the adiabatic reaction regime or very weak coupling of the quantum sub-system to the classical environment. In comparison between RPSH-CA and the conventional FSSH, inclusion of DBOC shows progressive deterioration in performance of the latter at reaction regimes corresponding to fast bath motions or as the reorganization energy increases.

Overall, considering the potential positive effect of including DBOC in RPSH-CA simulations, albeit with the observed system-dependent behavior, it is a parameter worth testing when dealing with different problems of interest. Therefore, these new developments are available for community use within the newest version of our user-friendly and highly parallelized software package, SHARP pack.⁷² Future research should be directed toward systematic improvement of the accuracy of RPSH simulations for both symmetric and asymmetric potentials. Improving the efficiency of the method using recently introduced techniques that allow convergence of real-time path integral simulations with a fraction of the number of beads⁷³ is another exciting research direction. Finally, with our interest in simulating charge transport dynamics in functional layered materials,^{74–78} we foresee an interface of the SHARP pack with our highly parallelized MD software package, DL_POLY Quantum.^{79,80}

SUPPLEMENTARY MATERIAL

The [supplementary material](#) provides details of the spin-boson model Hamiltonian; the discretization of the Debye spectral density; RPSH bead convergence tests of population and temperature; nonadiabatic hopping statistics; and the comparison of the population dynamics by FSSH, FSSH^D, and two different DBOC variants of RPSH-CA at the low temperature of 30 K.

ACKNOWLEDGMENTS

This research used resources from Bridges2 at Pittsburgh Supercomputing Center through allocation Grant Nos. PHY240170 and CHE200007 from the Advanced Cyberinfrastructure Coordination Ecosystem: Services & Support (ACCESS) program,⁸¹ which was supported by U.S. National Science Foundation under Grant Nos. 2138259, 2138286, 2138307, 2137603, and 2138296. The authors acknowledge the HPC center at NJIT for the use of computing resources and the support provided.

AUTHOR DECLARATIONS

Conflict of Interest

The authors have no conflicts to disclose.

Author Contributions

Dil K. Limbu: Formal analysis (equal); Investigation (equal); Methodology (equal); Software (equal); Validation (equal); Writing – original draft (equal). **Sandip Bhushal:** Data curation (equal); Formal analysis (equal); Investigation (equal); Validation (equal); Visualization (equal). **Diana M. Castañeda-Bagatella:** Data curation (equal); Formal analysis (equal); Investigation (equal); Validation (equal); Visualization (equal). **Farnaz A. Shakib:** Conceptualization (equal); Formal analysis (equal); Methodology (equal); Project administration (equal); Resources (equal); Supervision (equal); Writing – review & editing (equal).

DATA AVAILABILITY

The data that support the findings of this study are available within the article and its [supplementary material](#). All data presented in this work were generated using the SHARP Pack package, which is available for download at https://github.com/fashakib/SHARP_pack_2. The SHARP Pack documentation is also available on <https://sharppack.readthedocs.io/en/latest/>.

REFERENCES

- ¹R. P. Feynman, "Space-time approach to non-relativistic quantum mechanics," *Rev. Mod. Phys.* **20**, 367–387 (1948).
- ²R. Feynman, A. R. Hibbs, and D. F. Styer, *Quantum Mechanics and Path Integrals: Emended Edition* (Dover Publications, 2010).
- ³M. Parrinello and A. Rahman, "Study of an f center in molten kcl," *J. Chem. Phys.* **80**, 860–867 (1984).
- ⁴J. Cao and G. A. Voth, "The formulation of quantum statistical mechanics based on the Feynman path centroid density. II. Dynamical properties," *J. Chem. Phys.* **100**, 5106–5117 (1994).
- ⁵J. Cao and G. A. Voth, "The formulation of quantum statistical mechanics based on the Feynman path centroid density. III. Phase space formalism and analysis of centroid molecular dynamics," *J. Chem. Phys.* **101**, 6157–6167 (1994).
- ⁶J. Cao and G. A. Voth, "The formulation of quantum statistical mechanics based on the Feynman path centroid density. IV. Algorithms for centroid molecular dynamics," *J. Chem. Phys.* **101**, 6168–6183 (1994).
- ⁷S. Jang and G. A. Voth, "Path integral centroid variables and the formulation of their exact real time dynamics," *J. Chem. Phys.* **111**, 2357–2370 (1999).
- ⁸I. R. Craig and D. E. Manolopoulos, "Quantum statistics and classical mechanics: Real time correlation functions from ring polymer molecular dynamics," *J. Chem. Phys.* **121**, 3368–3373 (2004).
- ⁹I. R. Craig and D. E. Manolopoulos, "Chemical reaction rates from ring polymer molecular dynamics," *J. Chem. Phys.* **122**, 084106 (2005).
- ¹⁰I. R. Craig and D. E. Manolopoulos, "A refined ring polymer molecular dynamics theory of chemical reaction rates," *J. Chem. Phys.* **123**, 034102 (2005).
- ¹¹J. Cao and G. A. Voth, "A unified framework for quantum activated rate processes. I. General theory," *J. Chem. Phys.* **105**, 6856–6870 (1996).
- ¹²E. Geva, Q. Shi, and G. A. Voth, "Quantum-mechanical reaction rate constants from centroid molecular dynamics simulations," *J. Chem. Phys.* **115**, 9209–9222 (2001).
- ¹³R. Colleperdo-Guevara, I. R. Craig, and D. E. Manolopoulos, "Proton transfer in a polar solvent from ring polymer reaction rate theory," *J. Chem. Phys.* **128**, 144502 (2008).
- ¹⁴S. Habershon, D. E. Manolopoulos, T. E. Markland, and T. F. Miller III, "Ring-polymer molecular dynamics: Quantum effects in chemical dynamics from classical trajectories in an extended phase space," *Annu. Rev. Phys. Chem.* **64**, 387–413 (2013).
- ¹⁵T. J. H. Hele, M. J. Willatt, A. Muolo, and S. C. Althorpe, "Communication: Relation of centroid molecular dynamics and ring-polymer molecular dynamics to exact quantum dynamics," *J. Chem. Phys.* **142**, 191101 (2015).
- ¹⁶T. E. Markland and M. Ceriotti, "Nuclear quantum effects enter the mainstream," *Nat. Rev. Chem.* **2**, 0109 (2018).
- ¹⁷N. Ananth, "Path integrals for nonadiabatic dynamics: Multistate ring polymer molecular dynamics," *Annu. Rev. Phys. Chem.* **73**, 299–322 (2022).
- ¹⁸A. R. Menzelev, N. Ananth, and T. M. Miller III, "Direct simulation of electron transfer using ring polymer molecular dynamics: Comparison with semiclassical instanton theory and exact quantum methods," *J. Chem. Phys.* **135**, 074106 (2011).
- ¹⁹J. S. Kretchmer and T. F. Miller III, "Direct simulation of proton-coupled electron transfer across multiple regimes," *J. Chem. Phys.* **138**, 134109 (2013).
- ²⁰R. Kapral and G. Ciccotti, "Mixed quantum-classical dynamics," *J. Chem. Phys.* **110**, 8919 (1999).
- ²¹G. Hanna and R. Kapral, "Quantum-classical Liouville dynamics of nonadiabatic proton transfer," *J. Chem. Phys.* **122**, 244505 (2005).
- ²²S. E. Brown and F. A. Shakib, "Recent progress in approximate quantum dynamics methods for the study of proton-coupled electron transfer reactions," *Phys. Chem. Chem. Phys.* **23**, 2535–2556 (2021).
- ²³F. A. Shakib and G. Hanna, "An analysis of model proton-coupled electron transfer reactions via the mixed quantum-classical Liouville approach," *J. Chem. Phys.* **141**, 044122 (2014).
- ²⁴F. A. Shakib and G. Hanna, "New insights into the nonadiabatic state population dynamics of model proton-coupled electron transfer reactions from the mixed quantum-classical Liouville approach," *J. Chem. Phys.* **144**, 024110 (2016).
- ²⁵F. Shakib and G. Hanna, "Mixed quantum-classical liouville approach for calculating proton-coupled electron-transfer rate constants," *J. Chem. Theory Comput.* **12**, 3020–3029 (2016).
- ²⁶P. Shushkov, R. Li, and J. C. Tully, "Ring polymer molecular dynamics with surface hopping," *J. Chem. Phys.* **137**, 22A549 (2012).
- ²⁷F. A. Shakib and P. Huo, "Ring polymer surface hopping: Incorporating nuclear quantum effects into nonadiabatic molecular dynamics simulations," *J. Phys. Chem. Lett.* **8**, 3073–3080 (2017).
- ²⁸J. C. Tully and R. K. Preston, "Trajectory surface hopping approach to non-adiabatic molecular collisions: The reaction of H⁺ with D₂," *J. Chem. Phys.* **55**, 562–572 (1971).
- ²⁹J. C. Tully, "Molecular dynamics with electronic transitions," *J. Chem. Phys.* **93**, 1061–1071 (1990).
- ³⁰S. Hammes-Schiffer and J. C. Tully, "Proton transfer in solution: Molecular dynamics with quantum transitions," *J. Chem. Phys.* **101**, 4657–4667 (1994).
- ³¹C. D. Schwieters and G. A. Voth, "The semiclassical calculation of nonadiabatic tunneling rates," *J. Chem. Phys.* **108**, 1055–1062 (1998).
- ³²C. D. Schwieters and G. A. Voth, "Extension of path integral quantum transition state theory to the case of nonadiabatic activated dynamics," *J. Chem. Phys.* **111**, 2869–2877 (1999).
- ³³S. Jang and J. Cao, "Nonadiabatic instanton calculation of multistate electron transfer reaction rate: Interference effects in three and four states systems," *J. Chem. Phys.* **114**, 9959–9968 (2001).
- ³⁴P. Ehrenfest, "Bemerkung über die angehäherte gältigkeit der klassischen mechanik innerhalb der quantenmechanik," *Z. Phys.* **45**, 455–457 (1927).
- ³⁵J. R. Duke and N. Ananth, "Mean field ring polymer molecular dynamics for electronically nonadiabatic reaction rates," *Faraday Discuss.* **195**, 253–268 (2016).
- ³⁶X. Tao, P. Shushkov, T. F. Miller III, and I. T. F. Miller, "Path-integral iso-morphic hamiltonian for including nuclear quantum effects in non-adiabatic dynamics," *J. Chem. Phys.* **148**, 102327 (2018).
- ³⁷S. Ghosh, S. Giannini, K. Lively, and J. Blumberger, "Nonadiabatic dynamics with quantum nuclei: Simulating charge transfer with ring polymer surface hopping," *Faraday Discuss.* **221**, 501–525 (2020).
- ³⁸Y. Shakya, R. Welsch, L. Inhester, and R. Santra, "Capturing electronic decoherence in quantum-classical dynamics using the ring-polymer-surface-hopping-density-matrix approach," *Phys. Rev. A* **107**, 062810 (2023).
- ³⁹J. Lu and Z. Zhou, "Path integral molecular dynamics with surface hopping for thermal equilibrium sampling of nonadiabatic systems," *J. Chem. Phys.* **146**, 154110 (2017).

- ⁴⁰J. Lu and Z. Zhou, "Accelerated sampling by infinite swapping of path integral molecular dynamics with surface hopping," *J. Chem. Phys.* **148**, 064110 (2018).
- ⁴¹J. R. Mannouch and A. Kelly, "Toward a correct description of initial electronic coherence in nonadiabatic dynamics simulations," *J. Phys. Chem. Lett.* **15**, 11687–11695 (2024).
- ⁴²L. Wang, J. Qiu, X. Bai, and J. Xu, "Surface hopping methods for nonadiabatic dynamics in extended systems," *Wiley Interdiscip. Rev.: Comput. Mol. Sci.* **10**, e1435 (2020).
- ⁴³D. K. Limbu and F. A. Shakib, "Real-time dynamics and detailed balance in ring polymer surface hopping: The impact of frustrated hops," *J. Phys. Chem. Lett.* **14**, 8658–8666 (2023).
- ⁴⁴J. C. Tully, "Perspective: Nonadiabatic dynamics theory," *J. Chem. Phys.* **137**, 22A301 (2012).
- ⁴⁵A. V. Akimov and O. V. Prezhdo, "The pyxaid program for non-adiabatic molecular dynamics in condensed matter systems," *J. Chem. Theory Comput.* **9**, 4959–4972 (2013).
- ⁴⁶N. Shenvi, "Phase-space surface hopping: Nonadiabatic dynamics in a superadiabatic basis," *J. Chem. Phys.* **130**, 124117 (2009).
- ⁴⁷R. Gherib, I. G. Ryabinkin, and A. F. Izmaylov, "Why do mixed quantum-classical methods describe short-time dynamics through conical intersections so well? Analysis of geometric phase effects," *J. Chem. Theory Comput.* **11**, 1375–1382 (2015).
- ⁴⁸R. Gherib, L. Ye, I. G. Ryabinkin, and A. F. Izmaylov, "On the inclusion of the diagonal Born–Oppenheimer correction in surface hopping methods," *J. Chem. Phys.* **144**, 154103 (2016).
- ⁴⁹D. Chandler and P. G. Wolynes, "Exploiting the isomorphism between quantum theory and classical statistical mechanics of polyatomic fluids," *J. Chem. Phys.* **74**, 4078–4095 (1981).
- ⁵⁰H.-T. Chen and D. R. Reichman, "On the accuracy of surface hopping dynamics in condensed phase non-adiabatic problems," *J. Chem. Phys.* **144**, 094104 (2016).
- ⁵¹A. Jain, E. Alguire, and J. E. Subotnik, "An efficient, augmented surface hopping algorithm that includes decoherence for use in large-scale simulations," *J. Chem. Theory Comput.* **12**, 5256–5268 (2016).
- ⁵²C. Zhu, A. W. Jasper, and D. G. Truhlar, "Non-Born–Oppenheimer trajectories with self-consistent decay of mixing," *J. Chem. Phys.* **120**, 5543–5557 (2004).
- ⁵³J. Morelli and S. Hammes-Schiffer, "Surface hopping and fully quantum dynamical wavepacket propagation on multiple coupled adiabatic potential surfaces for proton transfer reactions," *Chem. Phys. Lett.* **269**, 161–170 (1997).
- ⁵⁴A. J. Leggett, S. Chakravarty, A. T. Dorsey, M. P. A. Fisher, A. Garg, and W. Zwerger, "Dynamics of the dissipative two-state system," *Rev. Mod. Phys.* **59**, 1–85 (1987).
- ⁵⁵H. Wang, M. Thoss, and W. H. Miller, "Systematic convergence in the dynamical hybrid approach for complex systems: A numerically exact methodology," *J. Chem. Phys.* **115**, 2979–2990 (2001).
- ⁵⁶N. Rekik, C.-Y. Hsieh, H. Freedman, and G. Hanna, "A mixed quantum-classical Liouville study of the population dynamics in a model photo-induced condensed phase electron transfer reaction," *J. Chem. Phys.* **138**, 144106 (2013).
- ⁵⁷X. Sun, H. Wang, and W. H. Miller, "Semiclassical theory of electronically nonadiabatic dynamics: Results of a linearized approximation to the initial value representation," *J. Chem. Phys.* **109**, 7064–7074 (1998).
- ⁵⁸M. A. C. Saller, A. Kelly, and J. O. Richardson, "On the identity of the identity operator in nonadiabatic linearized semiclassical dynamics," *J. Chem. Phys.* **150**, 071101 (2019).
- ⁵⁹H. Wang, X. Song, D. Chandler, and W. H. Miller, "Semiclassical study of electronically nonadiabatic dynamics in the condensed-phase: Spin-boson problem with Debye spectral density," *J. Chem. Phys.* **110**, 4828–4840 (1999).
- ⁶⁰M. Thoss, H. Wang, and W. H. Miller, "Self-consistent hybrid approach for complex systems: Application to the spin-boson model with Debye spectral density," *J. Chem. Phys.* **115**, 2991–3005 (2001).
- ⁶¹R. Templaar and D. R. Reichman, "Generalization of fewest-switches surface hopping for coherence," *J. Chem. Phys.* **148**, 102309 (2018).
- ⁶²A. Ishizaki and G. R. Fleming, "Theoretical examination of quantum coherence in a photosynthetic system at physiological temperature," *Proc. Natl. Acad. Sci. U. S. A.* **106**, 17255–17260 (2009).
- ⁶³S. J. Cotton and W. H. Miller, "The symmetrical quasi-classical model for electronically non-adiabatic processes applied to energy transfer dynamics in site-exciton models of light-harvesting complexes," *J. Chem. Theory Comput.* **12**, 983–991 (2016).
- ⁶⁴B. R. Landry, M. J. Falk, and J. E. Subotnik, "Communication: The correct interpretation of surface hopping trajectories: How to calculate electronic properties," *J. Chem. Phys.* **139**, 211101 (2013).
- ⁶⁵Y. Tanimura, "Numerically ‘exact’ approach to open quantum dynamics: The hierarchical equations of motion (HEOM)," *J. Chem. Phys.* **153**, 020901 (2020).
- ⁶⁶N. Lambert, T. Raheja, S. Cross, P. Menczel, S. Ahmed, A. Pitchford, D. Burgarth, and F. Nori, "QuTiP-boFiN: A bosonic and fermionic numerical hierarchical-equations-of-motion library with applications in light-harvesting, quantum control, and single-molecule electronics," *Phys. Rev. Res.* **5**, 013181 (2023).
- ⁶⁷J. R. Johansson, P. D. Nation, and F. Nori, "QuTiP: An open-source Python framework for the dynamics of open quantum systems," *Comput. Phys. Commun.* **183**, 1760–1772 (2012).
- ⁶⁸J. E. Runeson and J. O. Richardson, "Spin-mapping approach for nonadiabatic molecular dynamics," *J. Chem. Phys.* **151**, 044119 (2019).
- ⁶⁹Z. Liu, N. Lyu, Z. Hu, H. Zeng, V. S. Batista, and X. Sun, "Benchmarking various nonadiabatic semiclassical mapping dynamics methods with tensor-train thermofield dynamics," *J. Chem. Phys.* **161**, 024102 (2024).
- ⁷⁰G. Amati, J. R. Mannouch, and J. O. Richardson, "Detailed balance in mixed quantum–classical mapping approaches," *J. Chem. Phys.* **159**, 214114 (2023).
- ⁷¹S. Habershon and D. E. Manolopoulos, "Zero point energy leakage in condensed phase dynamics: An assessment of quantum simulation methods for liquid water," *J. Chem. Phys.* **131**, 244518 (2009).
- ⁷²D. K. Limbu and F. A. Shakib, "SHARP pack: A modular software for incorporating nuclear quantum effects into non-adiabatic dynamics simulations," *Software Impacts* **19**, 100604 (2024).
- ⁷³N. London and M. R. Momeni, "Real-time dynamics with bead-Fourier path integrals. I. Bead-Fourier CMD," *J. Chem. Phys.* **163**, 144123 (2025).
- ⁷⁴Z. Zhang, D. Dell'Angelo, M. R. Momeni, Y. Shi, and F. A. Shakib, "Metal-to-semiconductor transition in two-dimensional metal–organic frameworks: An *ab initio* dynamics perspective," *ACS Appl. Mater. Interfaces* **13**, 25270–25279 (2021).
- ⁷⁵Z. Zhang, D. S. Valente, Y. Shi, D. K. Limbu, M. R. Momeni, and F. A. Shakib, "In silico high-throughput design and prediction of structural and electronic properties of low-dimensional metal–organic frameworks," *ACS Appl. Mater. Interfaces* **15**, 9494–9507 (2023).
- ⁷⁶S. Akbar, Y. Shi, M. A. Sabuj, M.-Q. Zhao, and F. A. Shakib, "Structural and electronic response of Fe(II) Hofmann-type conjugated coordination polymers to spin crossover," *ACS Appl. Electron. Mater.* **7**, 5143–5152 (2025).
- ⁷⁷Y. Shi and F. A. Shakib, "Machine learning committee neural network potential energy surfaces for two-dimensional metal–organic frameworks," *J. Phys. Chem. C* **129**, 2222–2230 (2025).
- ⁷⁸D. Dell'Angelo, M. R. Momeni, S. Pearson, and F. A. Shakib, "Modeling energy transfer and absorption spectra in layered metal–organic frameworks based on a Frenkel–Holstein Hamiltonian," *J. Chem. Phys.* **156**, 044109 (2022).
- ⁷⁹N. London, D. K. Limbu, M. R. Momeni, and F. A. Shakib, "DL_Poly quantum 2.0: A modular general-purpose software for advanced path integral simulations," *J. Chem. Phys.* **160**, 132501 (2024).
- ⁸⁰N. London, D. K. Limbu, M. O. Faruque, F. A. Shakib, and M. R. Momeni, "DL_Poly quantum 2.1: A suite of real-time path integral methods for the simulation of dynamical properties and vibrational spectra," *J. Phys. Chem. A* **129**, 4015–4028 (2025).
- ⁸¹T. J. Boerner, S. Deems, T. R. Furlani, S. L. Knuth, and J. Towns, "ACCESS: Advancing innovation: NSF's advanced cyberinfrastructure coordination ecosystem: Services & support," in *Practice and Experience in Advanced Research Computing, PEARC '23* (Association for Computing Machinery, New York, NY, 2023), pp. 173–176.